Proceedings of the
Annual Stability Conference
Structural Stability Research Council
Atlanta, Georgia, April 21-24, 2026

Modern stability design approach for composite members: insights shaping the AISC 360-22 and future directions

Abdullah Alghossoon[1], Duaa Omoush[1], Amit Varma[2]

Abstract
The recent development and adoption of Appendix II in the AISC 360–22 Specification marks a pivotal shift in composite concrete-filled tube (CFT) design, initially targeting high-strength rectangular sections. This paper chronicles the research evolution that established the new design approach and its subsequent generalization across broader material strength and geometries. The transformation began with analytical and numerical studies of high-strength rectangular CFT (HS-RCFT) members, producing simplified, more accurate design equations that eliminate traditional section classifications (compact, noncompact, slender) while incorporating local and global stability in the interaction curves, culminating in Appendix II of AISC 360–22. Subsequent probabilistic evaluation demonstrated that these equations maintain a consistent and high level of reliability even when applied to conventional strength materials and supported increasing resistance factors to 0.9 for columns and beams, promoting economic design while adhering to a reliability index of 2.6. Current efforts are focused on addressing the absence of clear design guidance for circular CFTs (CCFTs) in AISC 360–22. Utilizing knowledge-guided AI and comprehensive databases, new partially mechanical-based strength equations were developed for CCFT compression and flexure. These results provided the basis for formulating axial–flexure interaction equations in a format consistent with the Appendix II provisions for RCFTs, resulting in a unified design framework and recommending resistance factors of $\phi_c = 0.85$ for columns and $\phi_b = 0.9$ for beams. This collected body of research provides a robust, simplified, and unified design approach ready for integration into the next iteration of the AISC Specification in 2027.

Keywords: AISC 360-22, Stability, Composite structures, Concrete-filled tube, Knowledge-guided AI, High-strength, Reliability analysis.

1. Introduction

Concrete-filled tube (CFT) members, consisting of steel tubes filled with concrete, are efficient composite elements that combine high strength, ductility, and constructability. The steel tube provides confinement to the concrete core, enhancing its compressive capacity, while the concrete infill delays local buckling of the steel tube (A. Alghossoon et al., 2023; Lai & Varma, 2018; Saleh et al., 2022). Owing to this synergistic behavior, CFTs are used in many applications, including high-rise buildings, bridges, and offshore structures (Liew et al., 2016; Zheng & Wang, 2018). Structural systems with CFTs are now integrated into many international design codes, such as the US code ("AISC 360-22 Specifications for Structural Steel Buildings," 2022) (AISC 360-22), European code (Standardization, 2004) (EC4), and Chinese code (50936-2014, 2014) (GB50936). Historically, these design codes primarily focused on CFTs constructed with conventional strength materials and imposed limitations on both material strengths and geometric properties, such as member and section slenderness ratios. However, the rapid advancements in material science have led to the widespread availability and use of high-strength steel (HSS) with yield strengths up to 1000 MPa and concrete compressive strength up to 120 MPa. These enhanced characteristics offer significant opportunities for more slender and economical designs, but their application necessitates updated and more comprehensive design guidance (A. M. Alghossoon, 2021). The AISC 360-22 Specification takes a step forward by introducing Appendix II for the design of high-strength concrete-filled members. Although the appendices are intended to offer alternative design approaches, the equations provided in Appendix II effectively end up being the only practical way to design high-strength CFT members, given the limitations in the main provisions.

On the other hand, Appendix II design equations are exclusively applicable to rectangular concrete-filled tube (RCFT) members, leaving a critical gap for circular concrete-filled tube (CCFT) members. The geometric and behavioral distinctions of circular sections, such as the prominent tri-axial confinement effect and unique stress distributions, mean that design solutions for rectangular sections cannot be directly applied to circular counterparts without specific modifications (A. Alghossoon et al., 2025b). This paper aims to describe the comprehensive process of modifying and extending the design equations for CFT members, starting from the foundational work on rectangular sections that informed AISC 360-22, and detailing the subsequent modifications to address the specific challenges and characteristics of circular sections. The objective is to connect the foundational research that led to the AISC 360–22 high-strength rectangular provisions with the current proposals aimed at unifying the code to include high-strength circular members.

2. Background on fiber-based model

2.1 A new design philosophy for rectangular CFT

The introduction of Appendix II in AISC 360–22 marked a paradigm shift in how composite members are designed. The traditional methodology required engineers to categorize cross-sections into compact, non-compact, or slender and impose restrictive limitations on material strength and member global slenderness. This categorical approach resulted in abrupt changes in predicted strength and constrained the use of high-strength materials and long CFT members. The development of high-strength CFT design equations began with the comprehensive research by Alghossoon and Varma, motivated by the advancement of construction material strength and prior experimental and numerical studies demonstrating significant reductions in flexural capacity with increasing member slenderness. Their research led to proposed design equations, which were later incorporated into Appendix II of the AISC 360-22 Specification.

The methodology for developing these RCFT design equations was primarily based on comprehensive parametric studies conducted using fiber-based finite element modeling in OpenSees software (Fig. 1). This advanced numerical approach utilized effective (phenomenological) stress-strain curves for both steel and concrete, which implicitly accounted for complex material behaviors such as steel yielding, steel local buckling, concrete cracking, crushing, and the confinement effect. The models were rigorously benchmarked and calibrated against existing experimental data, covering a wide range of parameters including member and section slenderness, section aspect ratio, and material strengths (steel yield strength up to 700 MPa and concrete compressive strength up to 103 MPa) (A. Alghossoon & Varma, 2023b, 2023a).

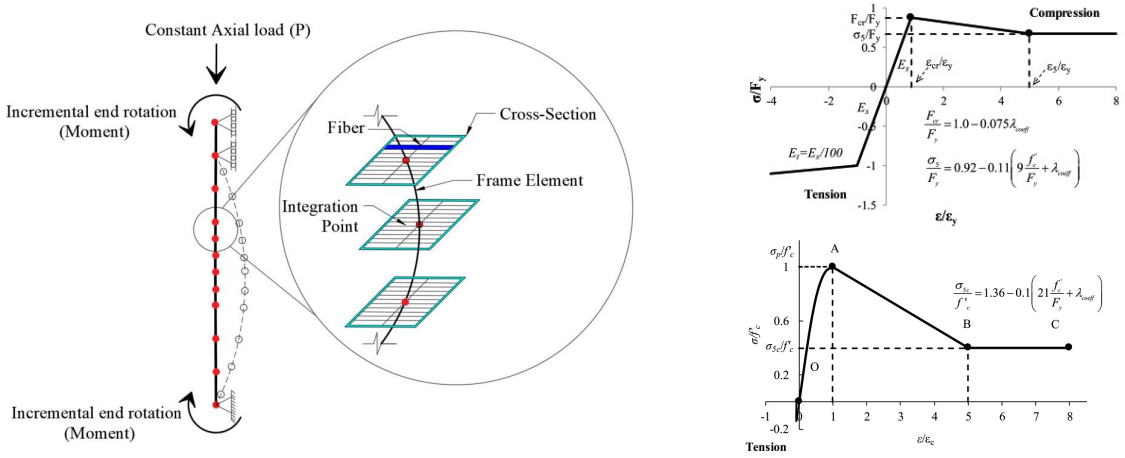

Figure 1: Fiber element modeling and effective stress-strain curve for steel and concrete in RCFT (A. Alghossoon & Varma, 2023a, 2023b)

2.2 Key features of the AISC 360-22 Appendix II include:

1- Elimination of section classification: The traditional requirement for classifying sections as compact, non-compact, or slender is removed. Instead, continuous functions were proposed to estimate the critical buckling strength of steel (F_n), which varies with the section slenderness ratio (λ). This continuous function is expressed as $F_n = F_y$ (1 - 0.075 λ).

2- Simplified stress blocks: The design approach employs simplified plastic stress distributions over the composite cross-section for calculating both axial and flexural strengths, as shown in Fig. 2. For axial compression, the nominal compressive strength (P_{no}) is the sum of the steel critical buckling strength and the infilled concrete strength.

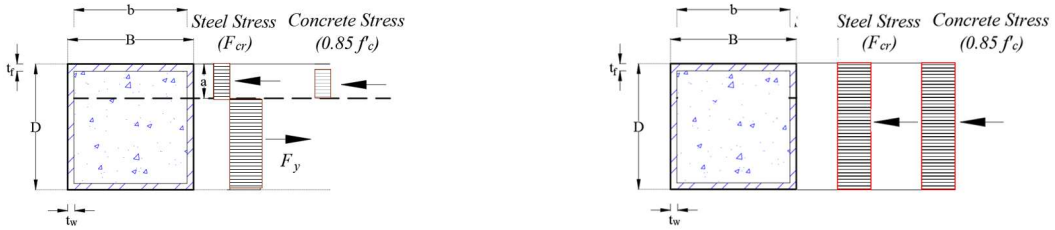

Figure 2: Stress blocks outlined in AISC 360-22 for estimating the nominal flexural and compressive strength (A. Alghossoon & Varma, 2023b)

3- Axial Compressive Strength: The traditional and well-established approach used in conventional column design is maintained using the cross-section capacity (P_{no}) in conjunction with the Euler buckling strength (P_e) to account for global stability.
4- Flexural Strength Reduction Factor: A reduction factor of 0.9 is applied to the flexural strength in the interaction equations. This is based on research demonstrating a 5%–10% reduction in flexural strength for slender members under high flexural stresses and modest axial loading, and is universally applied for simplicity due to considerations of accidental eccentricities.
5- Axial-Flexural (P-M) Interaction: Appendix II adopts simplified bi-linear interaction design equations for high-strength RCFT members (Fig. 3) while explicitly incorporating key parameters defining the curve balanced point, C_m and C_p, that were not considered in previous provisions, including member slenderness (P_n/P_{no}), section aspect ratio (B/D), and extended material strength.

$$\begin{cases} \dfrac{P_r}{P_c}+\dfrac{1-C_p}{C_m}\dfrac{M_r}{M_c}, For\ \dfrac{P_r}{P_c}\geq C_p \\ \dfrac{M_r}{M_c}+\dfrac{1-C_m}{C_p}\dfrac{P_r}{P_c}, For\ \dfrac{P_r}{P_c}< C_p \end{cases}$$

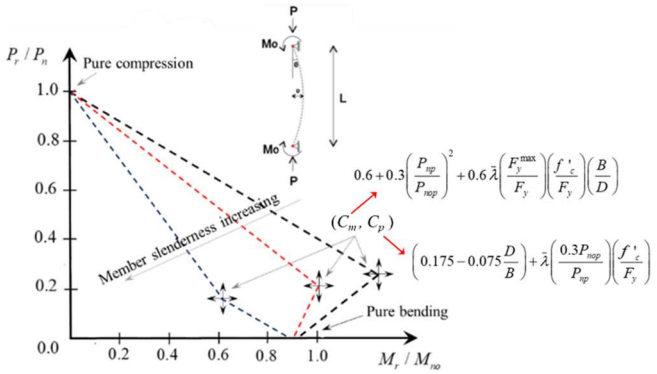

Figure 3: Mechanism of the bi-linear interaction curve (A. Alghossoon & Varma, 2023a)

Table 1 summarizes the key differences between the AISC 360-22 provisions in Chapter I and Appendix II for conventional and high-strength materials, respectively. Fig. 4 and Fig. 5 present schematic comparisons of the corresponding AISC 360-22 procedures for evaluating the compressive and flexural strengths of conventional and high-strength RCFT members, respectively.

Table 1: Comparison between Chapter I and Appendix II design equations in the AISC360-22

Criteria	**Chapter I (Conventional material strength)**	**Appendix II (High-strength material)**
Section classification (Compact, non-compact, slender)	Required	-
Global slenderness (L/D) or (P_n/P_{no})	-	Included
Local buckling (λ)	Included	Included
Section aspect ratio (D/B)	-	Included
Material strength	517 MPa for steel 70 MPa for concrete	690 MPa for steel 103 MPa for concrete

Conservatism	• Very conservative with slender sections and a high strength concrete-to-steel ratio • Significant unconservative error with slender member (global)	• Consistent level of conservatism • Accounts for global member slenderness

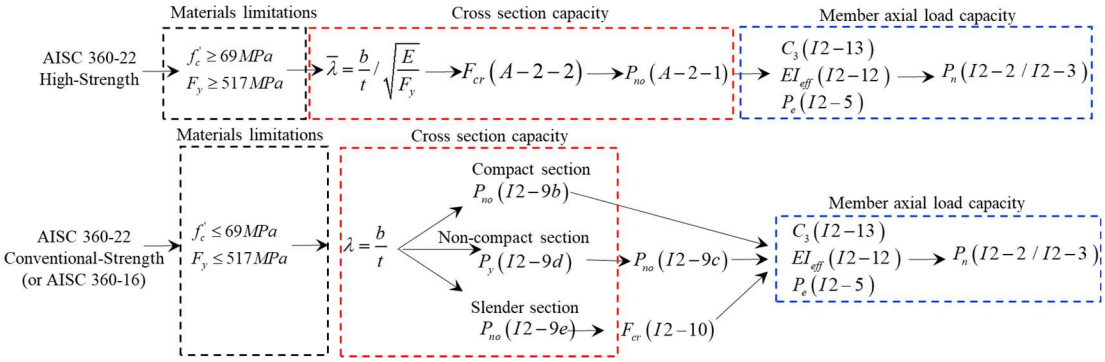

Figure 4: AISC 360-22 Procedure for determining compressive strength of RCFT columns. High-Strength vs. Conventional Strength materials (or AISC 360-16)

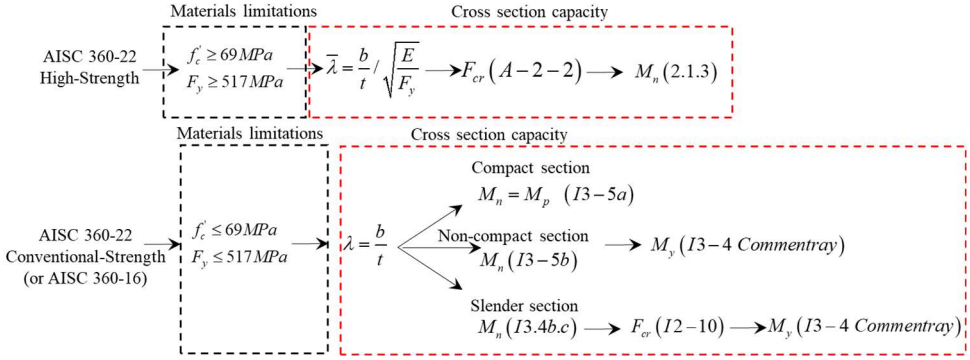

Figure 5: AISC 360-22 Procedure for determining flexural strength of RCFT beams. High-Strength vs. Conventional Strength materials (or AISC 360-16)

2.3 Toward a unified design equations: reliability-based assessment

Although being calibrated for high-strength materials, the RCFT design equations in Appendix II have been extensively evaluated using deterministic and probabilistic approaches and shown to provide more precise results even when applied with conventional material strength. These evaluations, shown in Fig. 6, demonstrate a consistent level of reliability, permitting a more relaxed resistance factor, outperforming conventional design equations (A. Alghossoon et al., 2024). This consistent performance supported the recommendation to extend their applicability to conventional-strength materials, thereby streamlining design practice. The current AISC 360-22 Specification continues to adopt the earlier resistance factors of 0.75 for columns and 0.9 for beams, even within Appendix II. While these factors have been historically accepted, they create an inconsistency in design outcomes. Specifically, under the existing provisions, a bare steel tube designed as a conventional steel section with a factor of 0.9 could theoretically exhibit a higher design strength than the same tube filled with concrete and designed using the lower factor of 0.75, a clearly counterintuitive result. Although further time may be needed to develop full confidence

with the current design equations across all practical scenarios, evidence from extensive deterministic and probabilistic evaluations of RCFT members indicates that a unified resistance factor of 0.9 for both columns and beams is both safe and rational (A. Alghossoon et al., 2024). Adopting this relaxed factor would not only correct the inconsistency in the code but also enable engineers to achieve more economical and efficient designs without compromising reliability.

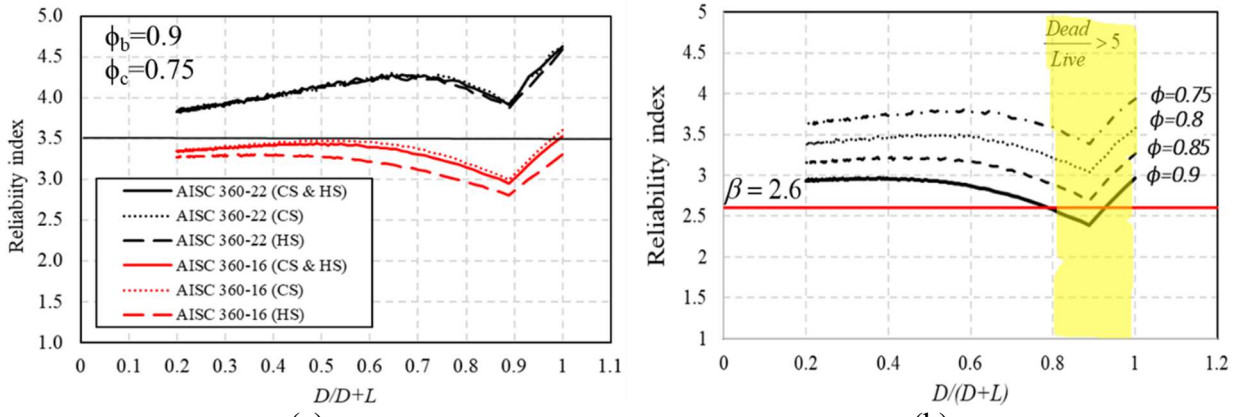

(a) (b)

Figure 6: Reliability index vs. load ratio for AISC 360-22 design equations for conventional (CH) and high-strength (HS) materials. (a) Beam-column behavior, (b) column behavior (A. Alghossoon et al., 2024)

3. Future directions: transitioning to circular CFT

3.1 Challenges and design limitations with circular sections

While rectangular provisions are now codified, circular concrete-filled tubes (CCFTs) continue to present distinct challenges that have delayed their incorporation into Appendix II. This gap comes from fundamental differences in geometric characteristics and structural behavior, which make a direct extension of rectangular CFT formulations neither straightforward nor reliable. As a result, guidance for circular sections remains limited and often ambiguous across current design codes, with many existing models either underestimating or overestimating member capacities by failing to adequately account for the interaction of section and member slenderness, an issue that becomes particularly critical when high-strength materials are used. Consequently, extending the AISC 360–22 Appendix II framework to CCFT members first requires identifying the key challenges that govern the behavior and design of circular sections, as summarized below:

1- Geometric Complexity: The continuous curvature introduces unique challenges for stress distribution calculations, complicating the derivation of closed-form solutions for flexural strength.
2- Confinement Effect: Circular steel tubes provide a more effective confinement to the concrete infill. This significantly enhances the concrete's compressive strength and ductility, while generating hoop stresses in the steel tube, reducing its effective yield strength and resulting in a more complex interaction behaviour.
3- Steel Local Buckling Behavior: While concrete infill generally restrains local buckling, its behavior in circular sections requires specific investigation. Traditional section classifications for circular hollow structural sections (HSS) were often conservatively applied to CCFTs due to a lack of dedicated research.
4- Limitations in Existing Standards: Existing design standards for CCFTs impose restrictive limits on material strengths and geometric properties, such as slenderness ratios (*L/D*, *D/t*), due to limited experimental and theoretical development.

3.2 Overcoming complexity with AI

Traditionally, design equations for structural members have been developed using deterministic and probabilistic approaches, often relying on non-linear regression to fit experimental and numerical data. While effective, these methods often fail to fully capture complex interactions or extrapolate beyond available datasets. In recent years, Artificial Intelligence (AI) has emerged as a powerful tool for structural engineering, capable of learning from large datasets and predicting structural behavior with high accuracy (A. Alghossoon et al., 2025c; Salehi & Burgueño, 2018). However, purely data-driven AI models are often viewed with skepticism by experienced engineers, as they may lack transparency and mechanistic interpretability, making them difficult to trust for practical design. To address this concern, a knowledge-guided AI approach was adopted for circular concrete-filled steel tubes (CCFTs). By integrating extensive experimental and numerical data with engineering insight and fundamental structural principles, the AI was guided to produce reliable, interpretable, and partially physics-based design equations, combining the predictive power of AI with the confidence of traditional engineering understanding (A. Alghossoon et al., 2025c).

3.3 Modification process for circular CFT (HS-CCFT) members

The development of the design equations for high-strength circular CFT members followed a deliberate and consistent path, building directly on the framework established for rectangular CFT sections. The modification process focused on formulating reliable expressions for axial compressive strength, flexural strength, and axial–flexure interaction, with the objective of achieving both technical rigor and practical clarity. Rather than reverting to traditional section classification schemes—where circular steel tubes are categorized as compact, noncompact, or slender—the proposed approach adopts a continuous functional representation to describe steel tube buckling behavior. This decision was intentional. Experience with rectangular CFT members demonstrated that discrete classifications introduce artificial boundaries, complicate design procedures, and often obscure the true structural response. By contrast, a continuous function captures the gradual evolution of local buckling effects in a physically meaningful manner, without abrupt shifts in predicted strength. By extending this same philosophy to circular CFT members, a unified and coherent design methodology was achieved across section geometries. The resulting equations provide a smooth transition between behavioral regimes, eliminate unnecessary ambiguity, and significantly simplify implementation. Most importantly, the proposed formulation aligns closely with the way practicing engineers think and design, offering a clear, consistent, and dependable set of tools for the design of high-strength circular CFT members (A. Alghossoon et al., 2025a, 2025c, 2025b).

3.3.1 Axial compressive strength (columns)

The development of design equations for CCFT columns focused on deriving simplified, partially mechanical-based equations that account for the unique interactions within circular sections. The proposed compressive strength of the circular cross-section (P_{nop}) was defined as the sum of the steel and concrete plastic strengths, incorporating factors that account for steel local buckling (C_1), bi-axial state of stresses on steel (C), and concrete confinement (C_c).

$$P_{nop} = C_c A_c 0.85 f_c^{'} + C A_s C_1 F_y \tag{1}$$

where P_{nop} is the proposed compression strength at the section level, C_c is the confinement coefficient, A_c is the area of concrete, f'_c is the concrete compressive strength, C is the biaxial state of stress, A_s is the area of steel, C_l is the local buckling coefficient, and F_y is the steel yield strength.

A significant finding was that steel local buckling is improbable for practical circular sections, even slender ones. This is attributed to the uniform stress distribution and substantial restraint provided by the adhered concrete. Consequently, a consistent factor of C_l= 1 was adopted across all scenarios, aligning with the observed absence of non-compact and slender composite sections in design manuals like AISC 360-22 for this failure mode. The presence of bi-axial stresses in the steel tube, resulting from the confinement of concrete, leads to a reduction in steel yield strength. This effect was accounted for with a reduction factor of approximately 10% (i.e., C ≈ 0.9). The confinement effect, a hallmark of circular CFTs, was meticulously addressed. New expressions for the confinement coefficient (C_c) were formalized to incorporate both the traditional confinement ratio ($\zeta = A_s F_y / A_c f'_c$) and the material modulus ratio ($\eta = E_s / E_c$). An example expression derived is $C_c = 2 (\zeta / \eta)^{0.2}$. This provided more reliable estimates of concrete confinement, bridging theoretical predictions with practical use, with confinement effects ranging between 0.8 and 2.3 (A. Alghossoon et al., 2025c).

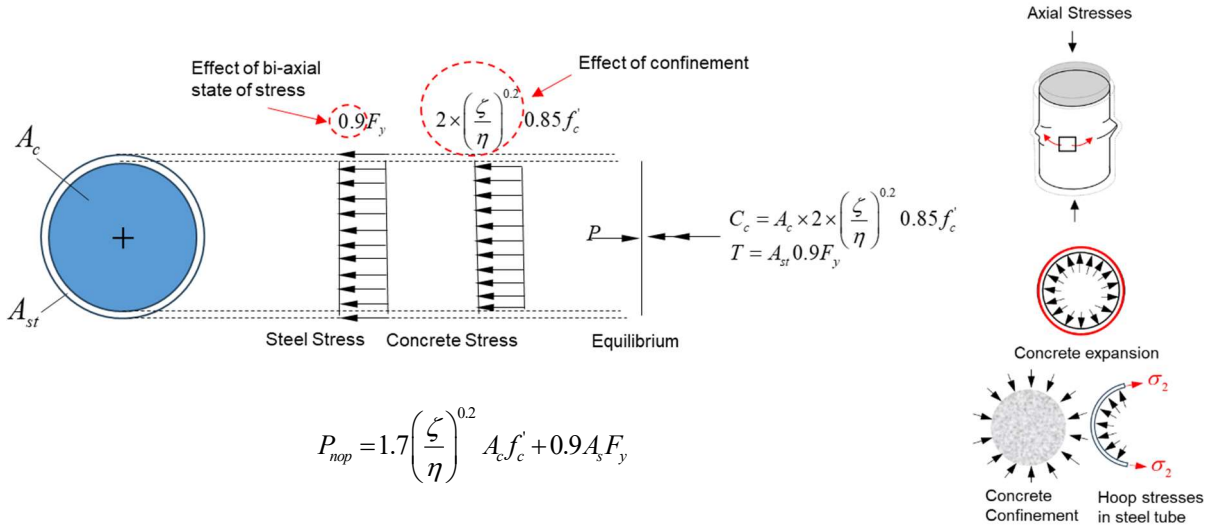

Figure 7: Proposed stress block for compressive strength of HS-CCFT columns (A. Alghossoon et al., 2025c).

The proposed plastic stress distribution method for CCFT columns eliminates the need for section classification, simplifying the design process while improving prediction accuracy. Once the section's nominal compressive strength (P_{nop}) was established, the AISC 360-22 column design curve (originally developed for rectangular sections) could be effectively adapted to account for member slenderness in circular sections by using the newly derived P_{nop} in conjunction with the Euler buckling strength (P_e) (A. Alghossoon et al., 2025c).

3.3.2 Flexural strength (beams)

Predicting the flexural strength of CCFT beams presented unique challenges due to the non-uniform stress distribution in circular shapes. The modification process involved developing a simplified approach using plastic stress blocks that satisfy equilibrium over the cross-section, which was proposed to determine the flexural strength of the CCFT section, as shown in Fig. 8.

These stress blocks incorporated the same factors for concrete confinement (C_c) and steel local buckling (C_l) derived from the column research. The uniform distribution of stresses for C_l =1 was assumed to simplify beam design while maintaining reasonable accuracy. The nominal moment capacity, M_{nop}, shown in Eq. 2, was determined as the sum of moments about the neutral axis resulting from concrete in compression (M_{cc}), steel in tension (M_{st}), and steel in compression (M_{sc}) (A. Alghossoon et al., 2025b).

$$M_{nop} = M_{cc} + M_{sc} + M_{st} \tag{2}$$

where M_{nop} is the proposed moment capacity of CCFT, M_{cc} is the moment due to concrete in compression, M_{sc} is the moment due to steel in compression, and M_{st} is the moment due to steel in tension.

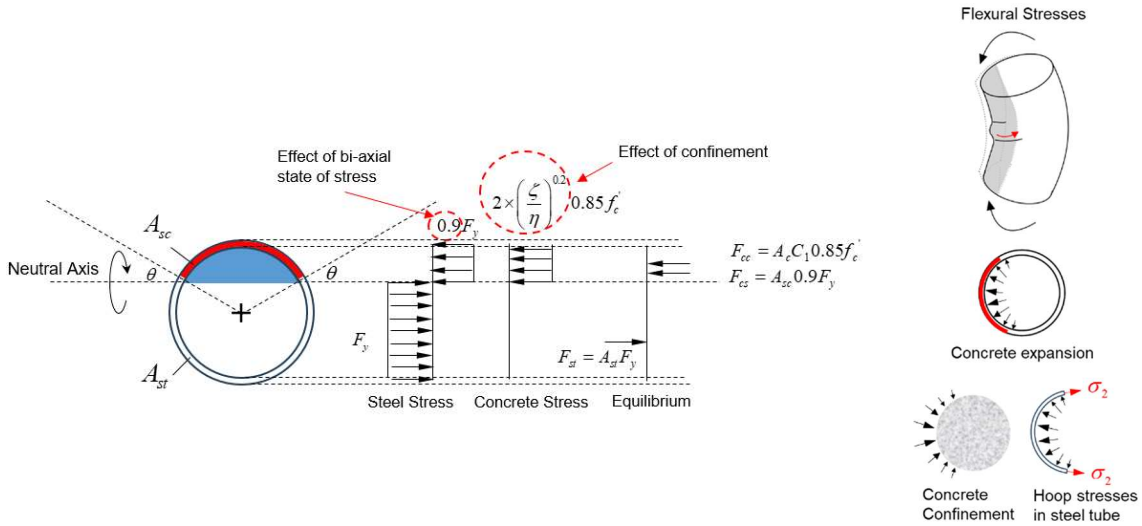

Figure 8: Developed stress block for flexural strength of CCFT beams (A. Alghossoon et al., 2025b).

The derivation of the neutral axis location is rigorously established in the author's paper through force and moment equilibrium. However, further examination revealed a significant correlation between the angular position of the neutral axis and the confinement ratio ζ, leading to the simplified expression shown in Eq. 3. The final expression for the predicted bending moment is shown in Eq. 4 (A. Alghossoon et al., 2025b).

$$\theta = 0.45 \times \zeta^{-0.3} \tag{3}$$

$$M_{nop} = 0.5 f_c' C_c \left(r_o \cos\theta\right)^3 + 4 F_y t r_o^{\,2} \cos\theta \tag{4}$$

where Θ is the angular location of the plastic neutral axis, ζ is the confinement ratio, r_o is the outer radius of cross section, and t is the steel tube thickness.

3.3.3 Axial-flexural interaction (beam-column)

The structural response of composite members in typical frame structures is governed by the interaction between axial force and flexural capacity. Rather than developing separate axial–flexural design equations for circular sections, the bi-linear axial–flexural interaction curve

adopted for RCFT members in Appendix II of the AISC 360-22 was retained to ensure consistency and avoid unnecessary complication (A. Alghossoon et al., 2024). Although this interaction formulation was originally derived for RCFT sections, it is grounded in fundamental principles of equilibrium and strain compatibility that are independent of cross-sectional geometry. Moreover, expressing the interaction relationship in normalized form using axial and flexural capacities, section-specific characteristics are embedded within the reference strengths rather than the interaction function itself. Accordingly, with only minor adjustments to account for geometric differences, Appendix II interaction equations can be extended and adapted for CCFT sections.

$$\begin{cases} \dfrac{P_r}{P_c}+\dfrac{1-C_p}{C_m}\dfrac{M_r}{M_c}, & for \quad \dfrac{P_r}{P_c}\geq C_p \\ \dfrac{M_r}{M_c}+\dfrac{1-C_m}{C_p}\dfrac{P_r}{P_c}, & for \quad \dfrac{P_r}{P_c}< C_p \end{cases} \tag{5}$$

$$C_m = 0.6+0.3\left(\frac{P_{np}}{P_{nop}}\right)^2+0.6\bar{\lambda}\left(\frac{F_y^{\max}}{F_y}\right)\left(\frac{f'_c}{F_y}\right) \tag{6}$$

$$C_p = 0.1+\bar{\lambda}\left(\frac{0.3P_{nop}}{P_{np}}\right)\left(\frac{f'_c}{F_y}\right) \tag{7}$$

where P_r is the applied compressive strength, P_c is the Design / allowable compressive strength = $\phi_c P_n$, P_n/Ω_c, respectively, M_r is the applied flexural strength, M_c is the Design / allowable flexural strength = $\phi_b M_n$, M_n/Ω_b, respectively, C_p and C_m is the balance point coordinates representing the normalized axial and flexural strength, respectively, and $F_y^{\max}$ equal 690 Mpa.

For circular shapes, the section aspect ratio (B/D) was set to 1 in the interaction equations for the balance point coordinates, C_m and C_p, while setion slenderness ratio $\bar{\lambda} = D/t\sqrt{E/F_y}$.

3.3.4 Reliability analysis and proposed factor of safety

To evaluate the adequacy and conservatism of the proposed design approach, a reliability analysis based on Monte Carlo simulation was conducted. In addition, the analysis aimed to investigate the feasibility of adopting more relaxed safety factors to achieve improved design economy while maintaining acceptable reliability levels consistent with current design practice. Uncertainties in material properties, geometric parameters, and loading conditions were explicitly modeled, and structural reliability was quantified in terms of the reliability index. The results were compared against commonly accepted target reliability levels, providing a rational basis for assessing whether reductions in safety factors can be justified without compromising structural safety. The probabilistic analysis demonstrated the adequacy of the proposed design equations by maintaining a minimum reliability index of 2.6 using the commonly governing load combination. The safety index versus load ratio curve in Fig. 9 demonstrates the applicability of using safety factors to ϕ_c = 0.85 for columns and ϕ_b = 0.9 for beams to reduce unnecessary conservatism while still aligning with AISC 360-22's requirement (A. Alghossoon et al., 2025a).

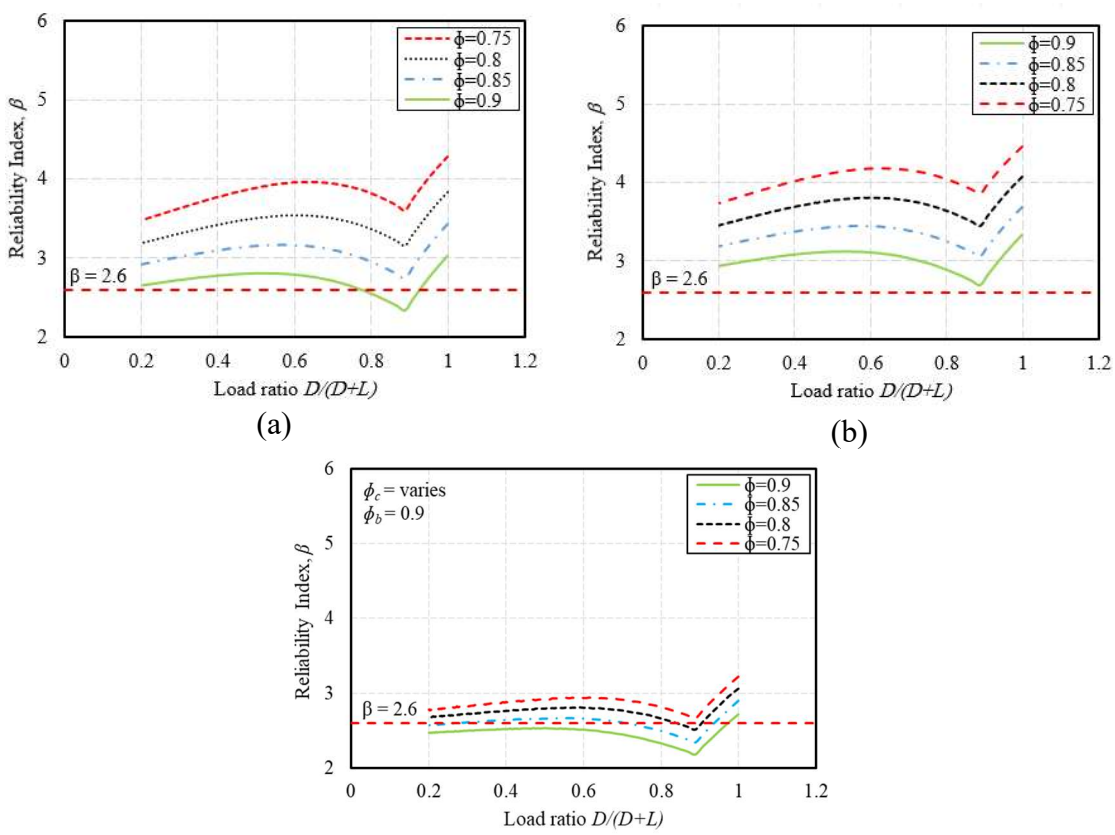

Figure 9: Reliability index vs. factor of safety for (a) column, (b) beam, and (c) beam-column (A. Alghossoon et al., 2025a)

4. Conclusions

This paper has documented the background, formulation, and rationale of the design equations currently included in Appendix II of AISC 360-22, while also presenting the future direction for extending these provisions to circular CFT sections, for which Appendix II equations are presently unavailable. Although Appendix II is explicitly referenced for high-strength rectangular CFT members, the Specification does not limit its application to conventional-strength materials. Furthermore, the Commentary encourages the use of Appendix II for slender members with *L/D* ratios exceeding 20, as well as for columns providing stability to leaning or heavily loaded gravity members, thereby supporting broader adoption of Appendix II provisions in practice.

The future direction is toward the inclusion of circular CFT sections in the next AISC provisions (AISC 360-27), along with a transition away from discrete section classifications, compact, noncompact, and slender, toward the use of continuous functions that directly account for section stability. Consistent with the current equations in Appendix II, the proposed design equations for circular sections explicitly incorporate the effects of global stability in their Bi-linear interaction curve, enabling safe and reliable design of slender columns. The cross-section strength expressions for circular CFT members were developed using knowledge-guided artificial intelligence techniques, which leverage established experimental observations and numerical results to generate closed-form equations while preserving the underlying physical behavior.

Based on the new findings and reliability analysis, the authors proposed adjusted and more relaxed safety factors that solve the inconsistent design outcomes, which sometimes result in bare steel section strength being more than the filled section, and promote more economical design.

References

50936-2014, G. B. (2014). *Technical code for concrete-filled steel tubular structures*. China Architecture & Building Press, Beijing.

AISC 360-22 Specifications for Structural Steel Buildings. (2022). *American Institute of Steel Construction*.

Alghossoon, A. M. (2021). *Analysis and Design of High-Strength Steel and Composite Members*. Purdue University.

Alghossoon, A., Omoush, D., & Varma, A. (2025a). AISC360-22 design equations for high-strength concrete-filled tubes: From rectangular to circular sections. *Journal of Constructional Steel Research*, *226*, 109148.

Alghossoon, A., Omoush, D., & Varma, A. (2025b). Flexural behaviour and design of circular concrete-filled tube beams: Effective stress method. *Engineering Structures*, *332*, 120104.

Alghossoon, A., Omoush, D., & Varma, A. (2025c). Modern techniques for designing high-strength circular concrete-filled tube columns: Knowledge-guided data approach. *Structures*, *78*, 109220.

Alghossoon, A., Tarawneh, A., Almasabha, G., Murad, Y., Saleh, E., & Sahawneh, H. (2023). Shear strength of circular concrete-filled tube (CCFT) members using human-guided artificial intelligence approach. *Engineering Structures*, *282*, 115820.

Alghossoon, A., Tarawneh, A., Hatamleh, M., & Alhusban, M. (2024). Generalizing AISC360–22's high-strength CFT member design equations for economical and safety-enhanced design. *Journal of Constructional Steel Research*, *215*, 108541.

Alghossoon, A., & Varma, A. (2023a). Beam-column behavior and design equations for high-strength composite filled tube (CFT) members: Investigating the interaction between section and member slenderness ratio. *Journal of Building Engineering*, *80*, 107943.

Alghossoon, A., & Varma, A. (2023b). Rectangular filled composite members made from high strength materials: behavior and design of columns and beams. *Thin-Walled Structures*, *185*, 110641.

Lai, Z., & Varma, A. H. (2018). High-strength rectangular CFT members: Database, modeling, and design of short columns. *Journal of Structural Engineering*, *144*(5), 04018036.

Liew, J. Y. R., Xiong, M., & Xiong, D. (2016). Design of Concrete Filled Tubular Beam-columns with High Strength Steel and Concrete. *Structures*, *8*, 213–226. https://doi.org/10.1016/j.istruc.2016.05.005

Saleh, E., Alghossoon, A., & Tarawneh, A. (2022). Optimal allocation of material and slenderness limits for the rectangular concrete-filled columns. *Journal of Constructional Steel Research*, *193*, 107283.

Salehi, H., & Burgueño, R. (2018). Emerging artificial intelligence methods in structural engineering. *Engineering Structures*, *171*, 170–189.

Standardization, E. C. for. (2004). EUROCODE 4, Design of composite steel and concrete structures-Part 1.1: General rules and rules for buildings. In *prEN 1994-1-1*.

Zheng, J., & Wang, J. (2018). Concrete-filled steel tube arch bridges in China. *Engineering*, *4*(1), 143–155.